Effect of an Energy Reservoir on the Atmospheric Propagation of Laser-Plasma Filaments

Shmuel Eisenmann,[1] Joseph Peñano,[2] Phillip Sprangle,[2] and Arie Zigler[1,3]
[1]*Racah Institute of Physics, Hebrew University, Jerusalem, Israel 91904*
[2]*Plasma Physics Division, Naval Research Laboratory, Washington, D.C. 20375, USA*
[3]*Icarus Research Inc., P.O. Box 30780, Bethesda, Maryland 20824, USA*
(Received 28 December 2007; published 17 April 2008)

The ability to select and stabilize a single filament during propagation of an ultrashort, high-intensity laser pulse in air makes it possible to examine the longitudinal structure of the plasma channel left in its wake. We present the first detailed measurements and numerical 3-D simulations of the longitudinal plasma density variation in a laser-plasma filament after it passes through an iris that blocks the surrounding energy reservoir. Since no compensation is available from the surrounding background energy, filament propagation is terminated after a few centimeters. For this experiment, simulations indicate that filament propagation is terminated by plasma defocusing and ionization loss, which reduces the pulse power below the effective self-focusing power. With no blockage, a plasma filament length of over a few meters was observed.

DOI: 10.1103/PhysRevLett.100.155003 PACS numbers: 52.38.Hb

Introduction.—The atmospheric propagation of high-intensity laser-plasma filaments and their various applications has attracted much attention in the past decade [1–4]. Filament propagation is usually explained as a self-guided structure achieved by a dynamic balance between Kerr self-focusing and plasma defocusing. As a result, a high-intensity laser filament is guided over many diffraction lengths (usually many meters) and leaves behind a plasma channel with a lifetime of several nanoseconds. During the filamentation process, bright spots corresponding to multiple filaments can be observed in the propagation path. In addition, one also observes a more diffused illuminated area or ''halo'' extending transversely well beyond the filaments. Since the energy in each filament is limited to approximately one mJ, for energetic laser pulses of duration ~100 fsec, most of the energy is contained in this halo. It is thought that the halo can act as an energy reservoir and play a very important role in the persistence of filament formation and regeneration over long distances [5]. It has been experimentally observed that filaments are regenerated when a central stopper blocks their propagation [6–8]. This property is interesting for applications where a large amount of laser energy must be propagated over extended distances through adverse atmospheric conditions such as fog or rain [9]. In other experiments, it was observed that a filament that passed though an iris which blocked the surrounding energy diverged after very short distances (a few centimeters), depending on the size of the hole [10]. It was hypothesized that the filament length is not determined only by ionization losses, but is due to the plasma defocusing, whenever the filament cannot be sustained by nonlinear focusing. However, this was never directly observed because the plasma density could not be directly measured. The main experimental difficulty is that the beam will break up into multiple filaments whenever the power of the laser beam is much higher than the critical power. The exact location of the filaments is dictated by the random noise of the initial beam. Thus, measuring the electron density along the propagation path of a single filament is not an easy task, since the filamentation pattern will differ from shot to shot. The exact location of the filaments is dictated by the random noise of the initial beam [11]

Recently, we have proposed a method for generating filamentation patterns which are stable from shot to shot [12]. This repeatability allows us to measure the plasma density of a particular laser-plasma filament at a specific location along the direction of laser propagation. In this Letter, we report the first measurement of electron density in a selected plasma filament after it passes through an iris that blocks the surrounding energy reservoir. We observe the formation of a high electron density filament after the iris which tends to defocus the high-intensity laser pulse. Analysis and simulations indicate, however, that ionization loss and pulse distortion caused by the iris also contribute to the termination of the filament. Since no compensation is available from the surrounding background energy, filament propagation is terminated after a few centimeters. The situation is markedly different from the case where no iris was used and filament propagation over a few meters was observed. Experimental results are found to be in good agreement with numerical 3-D simulations.

Experiment.—The experiment was conducted using a Ti:sapphire laser system capable of delivering a pulse as short as 100 fsec and energy up to 100 mJ at wavelength of 798 nm at 10 Hz repetition rate. The $1/e$ width of the beam intensity was 1 cm. The system was used to map the electron density variations that are left in the wake of a light filament as it propagates in air. We used a tilted lens configuration ($f = 5$ m) as described in Ref. [12] to create a stable filamentation pattern. A single filament was then directed between two thin copper wire electrodes (diameter

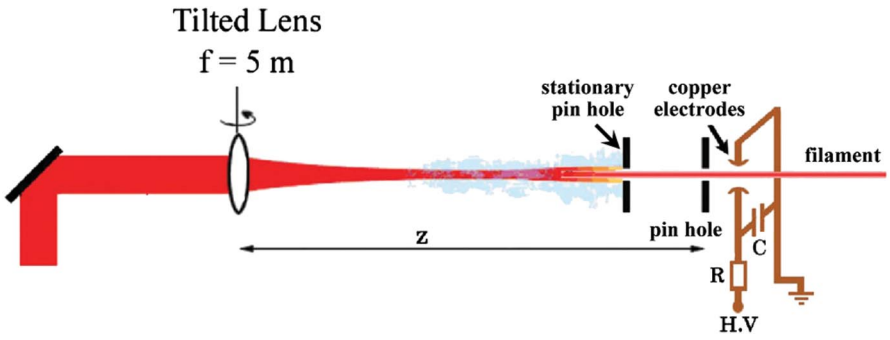

FIG. 1 (color). Schematic diagram of experimental setup.

of 0.5 mm) placed in the path of the light filament and perpendicular to its propagation direction. The electrodes spaced by 1.5 mm and charged to a voltage $V = 2$–5 kV. In order to prevent any photons from hitting the electrodes directly, which would result in the release of electrons from the electrode surface, and to make sure that only the monitored filament passes to the electrode gap, we placed a 500 μm aperture 1 cm before the electrodes. A schematic of the experimental setup is shown in Fig. 1. The method for deriving the longitudinal variation in electron density is explained in depth in our recent Letter [13]. Briefly, for each point, we measure the breakdown voltage V_0 between the electrodes without a plasma filament and then we measure the breakdown voltage V_f when a plasma filament is present between the electrodes. The generated free electrons act as a seed for breakdown. The ratio of these two voltages is a function of the initial electron density. By scanning along the length of the filament, we map the variation of electron density. This measurement technique gives us both high spatial resolution (limited by the size of the electrodes) and a range of at least 3 orders of magnitude in the electron density value, allowing us to observe the fine structure of the plasma filament.

We use the above technique to examine the effect of the energy-reservoir on the plasma filament. A 30 mJ laser pulse was sent through a tilted lens with a 5 m focus, and a single stabilized filament was obtained 300 cm from the lens. We first allowed the filament to propagate without obstruction. We scanned the entire length of the stabilized filament in steps of 2.5 cm and mapped its longitudinal plasma variation. Then, we placed an additional copper disk of diameter 2 cm with a 500 μm pinhole at its center 30 cm after the onset of filaments (see Fig. 1). The purpose of this stationary disk was to block the surrounding energy reservoir and allow mainly the filament core to propagate toward the electrodes. We then mapped the longitudinal plasma variation after the stationary pinhole. The results are presented in Fig. 2 where we plot the electron density as a function of propagation distance for the cases without the stationary pinhole [red curve in Fig. 2(a)] and with the stationary pinhole [red curve in Fig. 2(b)]. Results of our simulations, which will be discussed in the next Section, are plotted as the black curves in Fig. 2. The freely propagating filament shows variations in the electron density of an order of magnitude over relatively short distances (< 5 cm). The electron density along the entire detectable filament (few meters) varies almost 3 orders of magnitude. When the stationary disk is present, the rapid termination of the filament is evident.

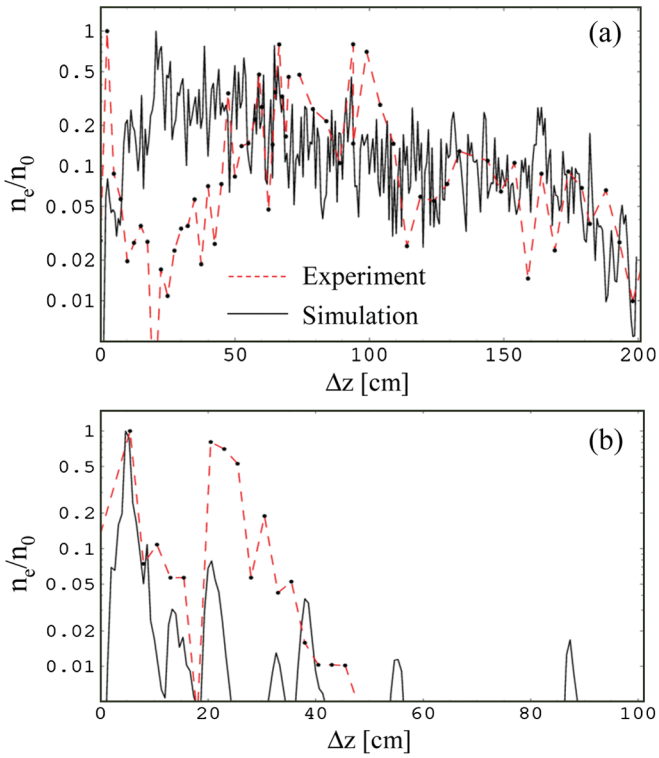

FIG. 2 (color). Simulated (solid black curve) and experimentally measured (dashed red curve) normalized electron density as a function of distance. Electron density, n_e, is normalized to the peak value, n_0. The distance is measured with respect to the onset of filamentation. Panel (a) shows the result of unapertured propagation, i.e., no stationary pinhole. Panel (b) shows the result for apertured propagation for a stationary pinhole diameter of 500 μm. For both cases, the laser pulse has a duration of 100 fsec (intensity FWHM), energy of 33 mJ, and a focal length of 5 m. A Gaussian laser pulse with a field spot size of $r_0 = 0.7$ cm was chosen for the numerical simulations.

Numerical simulations.—Filament dynamics of this experiment was simulated in 3D using the HELCAP code [14]. In the simulations, a laser pulse with a Gaussian profile in both time and space, e.g., $I \sim \exp(-2r^2/r_0^2)\exp(-2t^2/\tau^2)$ was propagated in air. The laser intensity was perturbed with a spectrum of white noise with ~5% amplitude to seed the formation of filaments. For the simulations, we chose a field spot size of $r_0 = 0.7$ cm, a pulse duration of $\tau = 85$ fsec, a peak power of 0.3 TW, and a focal length of 5 m. In the simulations, filamentation began after 3 m, which is in excellent agreement with the experimental observation. A single laser filament was formed on axis which then ionized the air and decayed into several filaments distributed randomly within the pulse. These filaments, in turn, decayed and others were reformed as the pulse propagated over a few meters. To simulate the experimental measurement technique, the plasma density was averaged over a circular area of diameter 500 microns centered on the pulse axis at various distances. The result is plotted as the solid black curve in Fig. 2(a), where the distance Δz is measured relative to the onset of filamentation, i.e., $z = 3$ m. The experimental measurement is plotted as the red, dashed curve. Both curves are normalized with respect to the peak electron density, which was $\sim 7 \times 10^{16}$ cm^{-3} in the simulation of Fig. 2(a) and $\sim 5.6 \times 10^{16}$ cm^{-3} for Fig. 2(b). There are apparent differences between the simulation and the experiment during the onset of filamentation ($\Delta z < 50$ cm). The experiment shows a relatively higher density in the formation of the first filament near $\Delta z = 0$. The observed density decrease of more than an order of magnitude at $\Delta z = 20$ cm is also not present in the simulation. However, there is excellent agreement between simulation and experiment for distances $\Delta z > 50$ cm. Both curves show fine scale (~ 1 cm) density variations of an order of magnitude. Also, apparent in both the simulation and experiment is a macroscopic trend in which the density decreases by an order of magnitude between $\Delta z = 50$ and 200 m.

We also simulated the effect of adding a pinhole just after filamentation onset. For these simulations, the laser intensity at radial positions greater than 250 microns was zeroed after the onset of filamentation. The density was then recorded as a function of z in the same manner as in Fig. 2(a). The result is shown in Fig. 2(b). It is seen that the stationary aperture limits filament propagation to <1 m. In these simulations, a single laser filament is formed initially, which then splits temporally to form two to three filaments. These laser filaments are defocused and refocused several times as the pulse propagates. The resulting plasma density behind the laser filaments is plotted in Fig. 2(b). No refocusing is observed after 90 cm of propagation. The experimental data [red dashed curve in Fig. 2(b)] shows filament propagation ending at 50 cm with a strong refocusing at ~22 cm similar to the simulation.

Discussion.—Filament propagation in this experiment is limited by a number of factors, the most important of which include laser energy loss due to ionization and plasma defocusing. In general, the plasma filament is terminated when the defocusing effects of the plasma and diffraction dominate the nonlinear self-focusing of the laser pulse. Energy loss due to ionization can cause the pulse power to become less than critical power for self-focusing, in which case self-focusing stops altogether, the laser pulse is defocused by the plasma, and the filament is terminated. Distortion of the laser pulse envelope by ionization can also enhance diffractive spreading and limit filament propagation, even when the pulse power is greater than the conventionally defined Kerr self-focusing power in air, i.e., $P_K = \lambda^2/(2\pi n_2)$, where n_2 is the optical Kerr index for air.

In the presence of plasma, a laser beam has an effective self-focusing power given approximately by [14]

$$P_{\mathrm{SF}} \approx \left[M^2 + \frac{2\pi\ell}{(\ell+1)^2} r_e R^2 n_{e0} \right] P_K, \qquad (1)$$

where M^2 is the conventional "times diffraction limited" beam quality parameter R, is the laser beam spot size, ℓ is the multiphoton ionization order, $r_e = e^2/mc^2$ is the classical electron radius, e is the electron charge, m is the electron mass, and n_{e0} is the electron density on axis. A beam with a transverse Gaussian profile has $M^2 = 1$, while non-Gaussian beams contain higher order modes and have $M^2 > 1$. The above expression for P_{SF} is valid for $M^2 \sim O(1)$. For typical laser-plasma filaments generated by a Ti:Sapphire laser, i.e., $n_{e0} \sim 5 \times 10^{16}$ cm^{-3}, $R \sim 100$ μm, and $\ell = 8$, the plasma contribution to P_{SF} can be comparable to the beam quality term, i.e., $2\pi\ell r_e R^2 n_{e0}/(\ell+1)^2 \sim 1$.

It is useful to examine the simulation of the apertured pulse in order to identify the mechanisms by which filament propagation is terminated. In the simulation, the pulse emerges from the 500 μm diameter stationary aperture with an energy of ~1.2 mJ and a peak power of ~18 GW. This value corresponds to ~5 times the Gaussian self-focusing power. After propagating 1 m, i.e., after the last ionization event observed in Fig. 2(b), the pulse has lost only 0.2 mJ to ionization. Its power is still 4 times greater than the Gaussian self-focusing power, yet no self-focusing occurs after 1 m in both the simulations and experiments. On the other hand, simulations run with the ionization energy loss artificially turned off resulted in much longer filament propagation. A possible explanation of these results is that the pulse emerging from the aperture is observed to be highly non-Gaussian in both the simulations and experiments. In the simulation of Fig. 2(b), for example, $M^2 \sim 6$ at the exit of the stationary pinhole. Hence, according to Eq. (1), the effective self-focusing power can be several times that of a Gaussian pulse. It is then possible that the small energy loss due to ionization (~ 0.2 mJ) was sufficient to reduce the pulse power below the effective self-focusing power and terminate the fila-

ment. These results also suggest that plasma defocusing cannot solely explain the termination of the filament since without ionization loss, the filament was observed to propagate much further.

The propagation of the unapertured pulse is much more complicated since many more filaments are formed both spatially and temporally. The onset and early phase of filamentation and plasma production is characterized by the formation of a few filaments which then decay into many finer scale filaments as the pulse propagates. The formation of the initial filaments is very sensitive to the initial laser pulse field, i.e., both intensity and phase, which is likely to differ significantly between simulation and experiment. This may account for the discrepancy in the microscale evolution of the density between the simulation and experiment in Fig. 2(a) for $\Delta z < 50$ cm. However, as filamentation progresses and many more filaments are formed, the pulse loses energy and the plasma density decays. This macroscopic decay of the plasma density is not strongly dependent on the evolution of individual filaments. Hence, provided that the ionization loss process is being modeled correctly, there should be good agreement between simulation and experiment with respect to the macroscopic decay of the plasma density, as is evident in Fig. 2(b).

Conclusions.—We have performed the first experimental measurement of the fine-scale longitudinal structure of an solitary laser-generated plasma filament and have compared the experimental measurements with 3D simulations. We have demonstrated that filament propagation is sustained by the surrounding laser energy reservoir. The propagation range of unapertured filaments was observed to be much greater than that of apertured filaments for which the majority of the surrounding laser energy is removed. It was also observed in simulations that the critical power for self-focusing is effectively increased relative to that of a Gaussian pulse. The increase in self-focusing power is mainly due to the non-Gaussian shape of the filament core after passing through the pinhole. Termination of the filament occurred when ionization loss reduced the laser power below this effective self-focusing power for a non-Gaussian filament.

The work was supported in part by *ISF No. 563-04 and the Office of Naval Research.

[1] J. Kasparian, M. Rodriguez, G. Mejean, J. Yu, E. Salmon, H. Wille, R. Bourayou, S. Frey, Y. Andre, A. Mysyrowicz, R. Sauerbrey, J. Wolf, and L. Wöste, Science **301**, 61 (2003).
[2] A. Couairon and A. Mysyrowicz, Phys. Rep. **441**, 47 (2007).
[3] R. Ackermann, G. Méjean, J. Kasparian, J. Yu, E. Salmon, and J.-P. Wolf, Opt. Lett. **31**, 86 (2006).
[4] L. Bergé, S. Skupin, R. Nuter, J. Kasparian, and J.-P. Wolf, Rep. Prog. Phys. **70**, 1633 (2007).
[5] M. Mlejnek, E. M. Wright, and J. V. Moloney, Opt. Lett. **23**, 382 (1998).
[6] F. Courvoisier, V. Boutou, J. Kasparian, E. Salmon, G. Méjean, J. Yu, and J.-P. Wolf, Appl. Phys. Lett. **83**, 213 (2003).
[7] A. Dubietis, E. Gaizauskas, G. Tamosauskas, and P. D. Trapani, Phys. Rev. Lett. **92**, 253903 (2004).
[8] M. Kolesik and J. Moloney, Opt. Lett. **29**, 590 (2004).
[9] G. Méchain, G. Méjean, R. Ackermann, P. Rohwetter, Y. André, J. Kasparian, B. Prade, Yu. J. Stelmaszczyk, E. Salmon, W. Winn, L. Schlie, A. Mysyrowicz, R. Sauberbrey, Wöste, and Wolf, Appl. Phys. B **80**, 785 (2005).
[10] W. Liu, F. Théberge, E. Arévalo, J.-F. Gravel, A. Becker, and S. L. Chin, Opt. Lett. **30**, 2602 (2005).
[11] V. I. Bespalov and V. I. Talanov, JETP Lett. **3**, 307 (1966).
[12] G. Fibich, S. Eisenmann, B. Ilan, and A. Zigler, Opt. Lett. **29**, 1772 (2004).
[13] S. Eisenmann, A. Pukov, and A. Zigler, Phys. Rev. Lett. **98**, 155002 (2007).
[14] P. Sprangle, J. R. Penãno, and B. Hafizi, Phys. Rev. E **66**, 046418 (2002).